BMC Cancer

RESEARCH

Open Access

Evaluating trophinin associated protein as a biomarker of prognosis and therapy response in renal cell carcinoma

Qinglin Tan[1†], Peiliang Kong[2†], Guobiao Chen[3†], Yanmin Cai[1], Kejun Liu[1], Chen Chen[1], Huiting Mo[1], Yuancheng Huang[1], Jianming Lu[4] and Yifen Wu[1*]

Abstract

Background Trophinin Associated Protein (TROAP) has been implicated in some tumors, yet its role in renal cell carcinoma (RCC) remains underexplored. This study aims to elucidate the prognostic and therapeutic implications of TROAP in RCC, encompassing different subtypes.

Methods Firstly, we identified the expression patterns of TROAP across various tumors within the TCGA pan-cancer cohort. Subsequently, the prognostic significance of TROAP was validated in three TCGA RCC cohorts and a local cohort. Finally, we conducted functional enrichment analysis, somatic mutations and copy number variations, assessed therapeutic response cohorts, and performed in vitro experiments to explore the biological characteristics of TROAP.

Results TROAP serves as an unfavorable factor in both the TCGA RCC datasets and our local cohort. Functional enrichment analysis and in vitro experiments have demonstrated its oncogene effect in promoting tumor progression. Additionally, the relationship between TROAP expression and gene mutations in RCC appears to be limited. Furthermore, elevated TROAP expression is associated with reduced efficacy of RCC therapies, including nivolumab and everolimus.

Conclusions Our findings illustrate TROAP as a pivotal biomarker for prognosis and therapeutic response in RCC. Elevated TROAP expression is indicative of aggressive tumor behavior and resistance to conventional therapies, making it a valuable target for personalized treatment strategies in RCC management.

Keywords Trophinin associated protein, Renal cell carcinoma, Prognosis, Therapy response, Immunotherapy

†Qinglin Tan, Peiliang Kong and Guobiao Chen contributed equally to this work.

*Correspondence:
Yifen Wu
31200195@smu.edu.cn
[1]Department of Oncology, Dongguan Key Laboratory of Precision Diagnosis and Treatment for Tumors, Dongguan Institute of Clinical Cancer Research, The Tenth Affiliated Hospital of Southern Medical University (Dongguan people's hospital), Dongguan 523059, China
[2]Department of Pulmonary & Critical Care Medicine, The Tenth Affiliated Hospital of Southern Medical University (Dongguan People's Hospital), Dongguan 523059, China
[3]Department of Thoracic Surgery, The Tenth Affiliated Hospital of Southern Medical University, Dongguan People's Hospital), Dongguan 523059, China
[4]Center for medical research on innovation and translation, Institute of Clinical Medicine, Guangzhou First People's Hospital, School of Medicine, South China University of Technology, Guangzhou 510180, China

Introduction

Renal cell carcinoma (RCC) is identified as the third most common urologic malignancy and ranks eighth in overall global cancer prevalence [1]. Annually, it is responsible for initiating over 400,000 new cases and contributes to approximately 175,000 fatalities worldwide [2, 3]. Histological and genetic examinations reveal various RCC subtypes. This investigation primarily addresses three widespread subtypes: renal clear cell carcinoma, chromophobe renal cell carcinoma and papillary renal cell carcinoma [4]. Notably, renal clear cell carcinoma emerges as the predominant subtype, comprising about 70% of all RCC cases [5, 6].

Over the last decade, advancements in the management of RCC have been substantial, leading to the incidental detection of many small renal tumors during routine screenings. Despite these improvements, approximately 17% of patients present with distant metastases at the time of diagnosis [7, 8]. Currently, surgical intervention remains the principal therapeutic approach for renal clear cell carcinoma [4]. In cases of advanced kidney cancer where surgery is not viable, molecularly targeted therapies have been employed to prolong life; however, these treatments are effective in only 30% of cases [9, 10]. Consequently, there is a pressing necessity to delve into the pathogenesis of RCC to unearth potential biomarkers that could aid in prognosis and therapeutic response monitoring.

Trophinin-associated protein (TROAP), also referred to as tastin, plays a crucial role in maintaining centrosome integrity and orchestrating spindle assembly during mitosis [11]. Composed of 778 amino acids, TROAP is a cytoplasmic protein enriched in proline and features three homologous domains [12]. It is encoded by the human TROAP gene located on chromosome 12q13.12 [13]. Initially, researchers identified TROAP's association with bystin and trophinin, proteins implicated in the early adhesion processes between blastocysts and uterine epithelial cells, potentially forming complexes critical for embryo implantation [14]. In the context of KIRC, TROAP is suspected to enhance tumor proliferation, migration, and metastasis through interaction with STAT3 [15]. Nevertheless, a comprehensive understanding of TROAP's prognostic significance and its role in pan-RCC remains elusive.

Materials and methods

Public data sources

TCGA-KIRC (renal clear cell carcinoma), TCGA-KIRP (papillary renal cell carcinoma) and TCGA-KICH (chromophobe renal cell carcinoma) Level 3 high-throughput RNA sequencing data, mutation data, and clinical information were acquired from the UCSC XENA platform (https://xenabrowser.net/datapages/). The advanced RCC cohorts were derived from previously published studies [16].

Pan-cancer evaluation

We utilized the R package "TCGAplot" (version 4.0.0) [17], which integrates expression profiles and follow-up information from the TCGA Pan-Cancer cohort. This package enabled us to perform differential expression analysis of TROAP in both non-matched and matched samples within the Pan-Cancer dataset, using the Wilcoxon test for statistical validation. Additionally, we conducted Cox regression analysis to evaluate the prognostic significance of TROAP.

Prognostic analysis

To evaluate the prognostic significance of TROAP, we utilized the R packages "timeROC" (0.4), "survival" (3.5-5) (https://CRAN.R-project.org/package=survival) and "survminer" (0.4.9). These tools were used to calculate the area under the receiver operating characteristic (ROC) curve (AUC), and to perform Cox regression and Kaplan-Meier (KM) analyses. For the KM survival analysis, TROAP expression levels were categorized as high or low based on the optimal cut-off value.

Functional enrichment

We assessed the correlation between TROAP expression and other mRNA expressions using correlation analysis. The "clusterProfiler" R package (version 4.8.1) [18] was employed for Gene Set Enrichment Analysis (GSEA) to perform functional enrichment.

Immunohistochemistry

In this study, RCC tissue samples were obtained from Shanghai Zhuoli Biotech Company. The tissue microarray (HKid-CRCC150CS-01) consisted of a total of 148 valid samples derived from patients diagnosed with KIRC. This tissue microarray includes 74 cases of KIRC and 74 matched normal tissue adjacent to the tumor (NAT). The collection of tissue samples was ethically approved by the Ethics Committee of Shanghai Zhuoli Biotech Company (SHLLS-BA-22101102). Prior to embedding in paraffin, samples were fixed in 4% formaldehyde. Each tissue block was sectioned into 4 μm thick slices, treated with a 1% H2O2 solution, and blocked with non-immunogenic goat serum. The sections were incubated overnight at 4 °C with primary antibodies, followed by a 30-minute room temperature incubation with biotinylated secondary antibodies to bind to the primary antibodies. The specific immunohistochemistry (IHC) staining procedure was consistent with our previous studies [19]. Scoring for immunoreactive cells was based on the percentage of positive staining cells and the intensity of staining, calculated by adding the percentage score and the intensity

score. The scoring for the percentage of immunoreactive cells was defined as follows: 0 (0%), 1 (1–10%), 2 (11–50%), and 3 (>50%). Staining intensity was visually scored and categorized as follows: 0 (negative), 1 (weak), 2 (moderate), and 3 (strong). The antibody used was an anti-TROAP antibody (Novus Biologicals, NBP1-92532).

Immune cell infiltration

The immune cell infiltration in TCGA-KIRC, TCGA-KIRP, and TCGA-KICH datasets was analyzed using the "IOBR" R package (version 0.99.9) [20]. Specifically, we employed the xCELL algorithm within the "IOBR" package to compute Type 2 T helper (Th2) cell scores for each sample. Spearman correlation analysis was then performed to evaluate the relationship between TROAP expression and Th2 cell infiltration.

Western blotting

Cell lysates were generated by harvesting cells and lysing them in RIPA buffer supplemented with protease inhibitors. Proteins from these lysates were separated using SDS-PAGE and then transferred onto PVDF membranes. These membranes were initially blocked using 5% non-fat milk before being incubated with a primary anti-TROAP antibody (Novus Biologicals, NBP1-92532) a, followed by incubation with an anti-β-ACTIN-Rb secondary antibody (Novus Biologicals). Subsequent to antibody binding, the membranes were washed three times in PBST, each wash lasting 10 min, in preparation for detection. β-ACTIN, utilized as a normalization control, was also added at a 1:5000 dilution (Novus Biologicals). The intensities of the protein bands were quantified using Image J software.

Cell culture and transfection

The Caki-1 and 786-O cell lines were acquired from Beina Chuanglian Biotechnology Institute (Beijing, China). Prior to use, all cell lines underwent mycoplasma testing and were authenticated via short tandem repeat (STR) profiling. The cells were maintained at 37 °C in an atmosphere containing 5% CO_2. Transfections were executed with GP-transfect-Mate (GenePharma, Suzhou, China), adhering to the supplied protocol [21]. Both a negative control (NC) and TROAP-specific siRNA (Table S1, Ribobio, Guangzhou, China) were introduced to the RCC cells as per the experimental design.

Cell counting Kit-8 assay

A 96-well plate was set up with roughly 4,000 cells that had been transiently transfected. This setup was replicated across five wells for each condition. The cells were incubated for time intervals of 2, 24, 48, and 72 h, after which 100 μL of a 1:9 dilution of CCK-8 solution in culture medium was administered to each well. Following an additional incubation period of 2 h, the optical density (OD) was measured at 450 nm using a spectrophotometer to assess cell viability.

Cell migration assay

To evaluate cell migration, we seeded about 40,000 transiently transfected cells in the upper chamber of a transwell apparatus using serum-free medium, while the lower chamber was filled with complete medium. The cells were incubated at 37 °C in an environment containing 5% CO_2 for a duration of 48 h. Post-incubation, cells were washed with saline, fixed with paraformaldehyde, and stained with 0.1% crystal violet. The stained cells were then visualized and quantified using microscopy.

Colony formation assay

Cells were plated at a density of 1,000 cells per well in 6-well plates and incubated at 37 °C with 5% CO_2 for a period of two weeks. Upon completion of the incubation period, the colonies were rinsed twice with cold phosphate-buffered saline (PBS), fixed using 4% paraformaldehyde for 15 min, and subsequently stained with 1% crystal violet for 20 min at ambient temperature. After staining, the colonies that were clearly visible were enumerated.

Mutation analysis

We utilized the R package 'maftools' to explore potential differences in gene mutation profiles between high and low TROAP expression groups [22]. This analysis allowed us to quantitatively assess the genomic variations and understand the mutational landscape associated with varying levels of TROAP expression.

Statistical analysis

Spearman's method was employed for correlation assessments, while continuous variables were compared using the Wilcoxon rank-sum test. Categorical variables were analyzed using either the Chi-squared test or Fisher's exact test as appropriate.

Results

Expression profile of TROAP across various tumor

As depicted in Fig. 1A, within the TCGA pan-cancer dataset, TROAP exhibits varying expression patterns across different cancer types. Notably, in three subtypes of RCC, TROAP is consistently expressed at higher levels in cancerous tissues. This phenomenon is similarly observed in matched samples from the TCGA pan-cancer dataset (Fig. 1B). Additionally, we observed that TROAP expression is higher in all cancer tissues compared to normal tissues. However, overall, its expression level in RCC is lower than in most other cancer types.

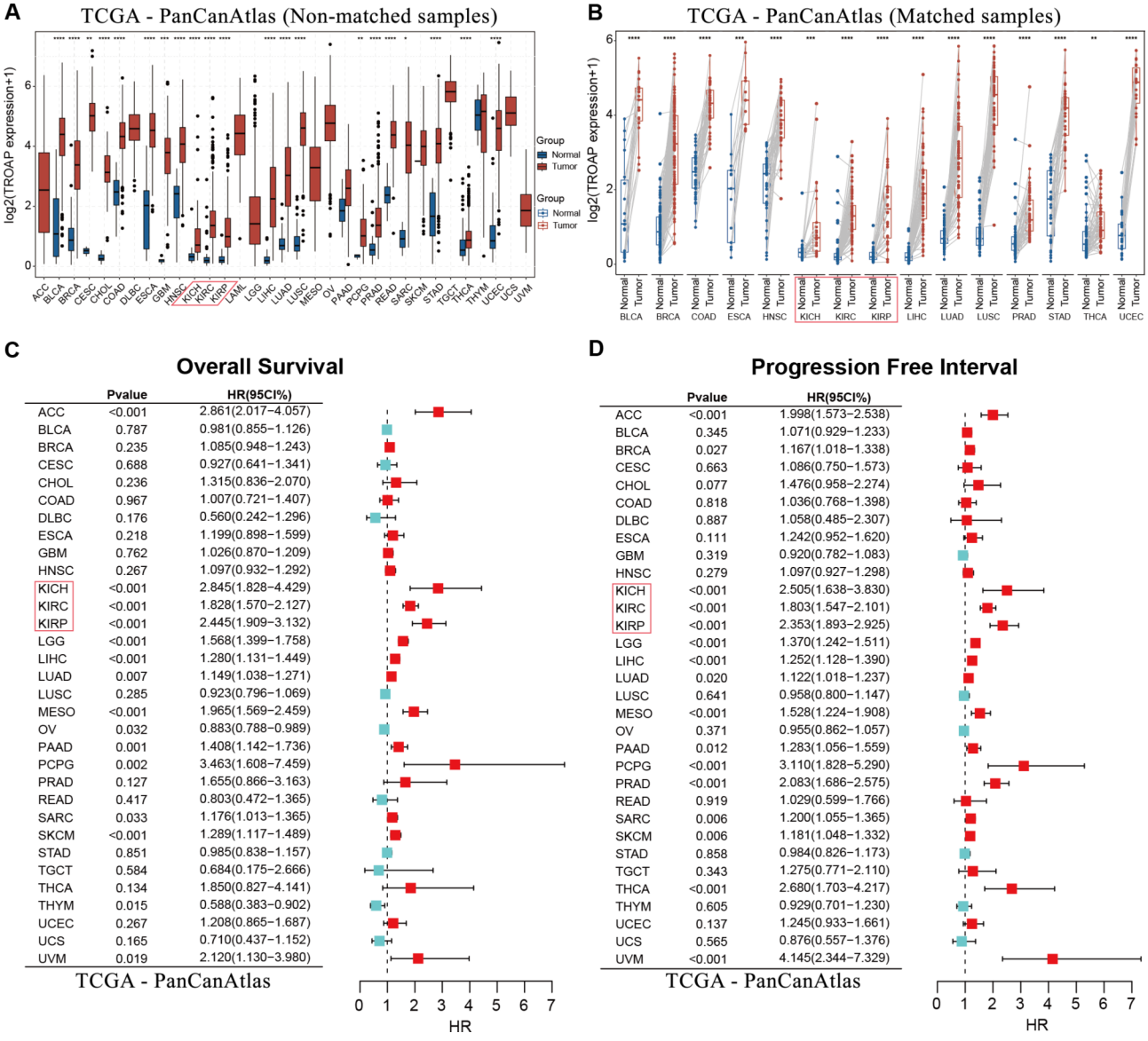

Fig. 1 Expression Pattern of TROAP in The Cancer Genome Atlas. (**A**) Differential analysis of TROAP in unmatched normal and cancer tissues. (**B**) Differential analysis of TROAP in matched normal and cancer tissues. Cox regression analysis reveals the prognostic value of TROAP in pan-cancer, (**C**) Overall Survival, (**D**) Progression Free Interval. *$p<0.05$; **$p<0.01$; ***$p<0.001$, **** $p<0.0001$; NS, No Significance

Moreover, in pan-cancer prognostic analysis using either Overall Survival (OS) or Progression Free Interval (PFI) as endpoints, TROAP is associated with poor prognosis in RCC (Fig. 1C-D). These findings suggest that TROAP holds considerable potential as a biomarker for RCC. Furthermore, TROAP serves as an adverse prognostic factor in most cancer types, except for ovarian cancer (OV) and thymoma (THYM), where it acts as a protective factor ($P<0.05$).

TROAP is an adverse prognostic factor for RCC

Initially, to evaluate the prognostic relevance of TROAP in RCC, we conducted Kaplan-Meier survival analysis, AUC assessments, and Cox regression analysis across KIRC, KICH, and KIRP subtypes. As illustrated in Fig. 2A, using KICH as an example, we observed that patients grouped by high expression of TROAP had poorer outcomes in Kaplan-Meier survival analysis with OS and PFI as endpoints. Furthermore, the ROC analysis at three time points consistently showed AUC values exceeding 0.7. Subsequent univariate and multivariate Cox regression analyses confirmed that elevated TROAP expression serves as an independent prognostic risk factor in KICH (Fig. 2A, Table S2). Similar patterns were also noted in KIRC and KIRP, although some ROC AUC values in KIRC were slightly below 0.7 (Fig. 2B-C, Table S2). These findings conclusively establish TROAP as an independent adverse prognostic factor in RCC.

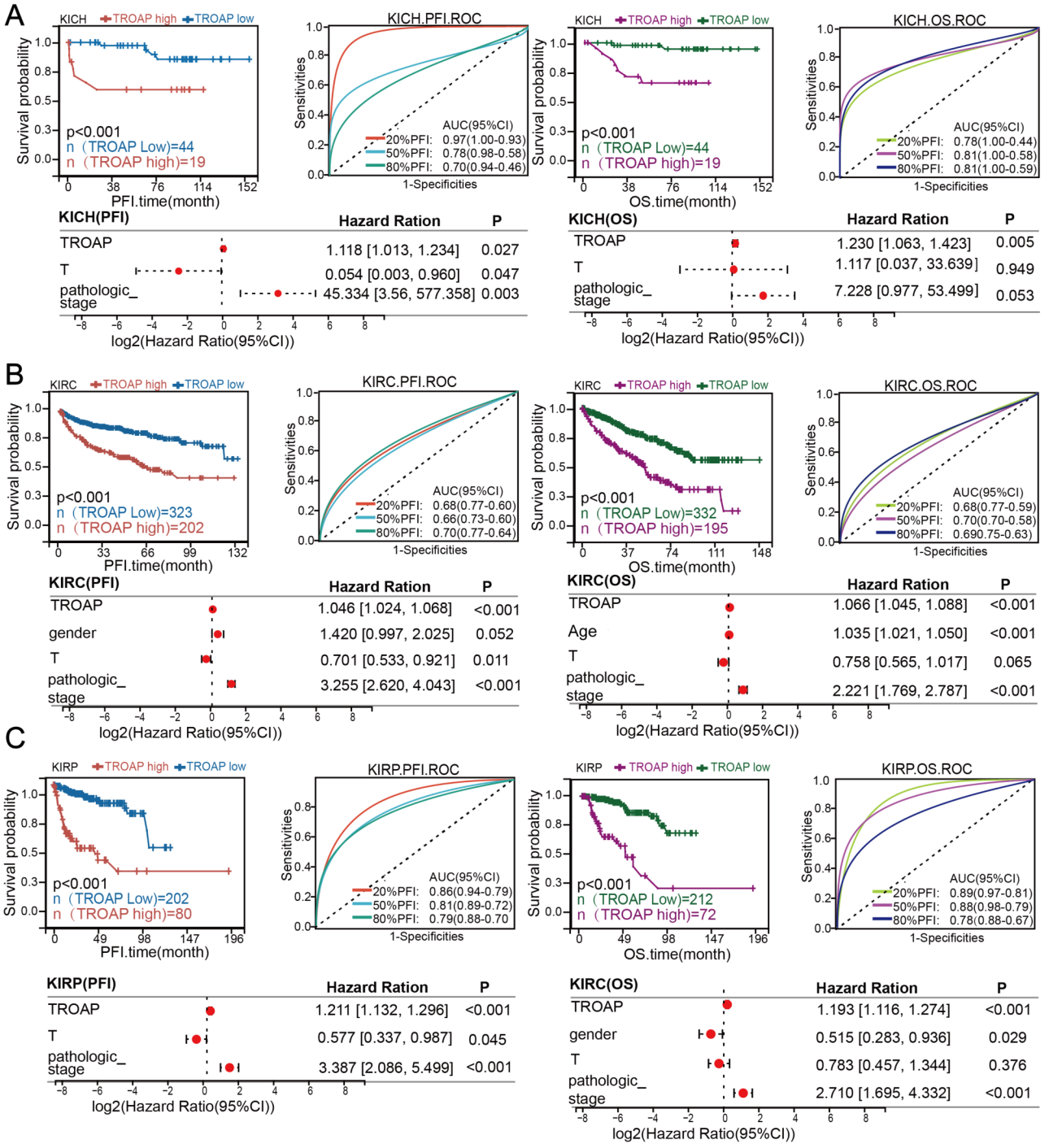

Fig. 2 Prognostic Value of TROAP in RCC. Kaplan-Meier survival analysis, time-dependent ROC, and multivariate Cox regression analysis, (**A**) chromophobe renal cell carcinoma, (**B**) renal clear cell carcinoma, (**C**) papillary renal cell carcinoma

Immunohistochemistry in local cohort

Subsequently, in our local cohort of KIRC, we conducted immunohistochemistry to corroborate findings from public datasets. The prognostic utility of TROAP in KIRC was further investigated using a tissue microarray. As depicted in Fig. 3A and B, TROAP was predominantly located in the cytoplasm. Upon evaluating the local cohort, we observed that TROAP expression was significantly higher in cancer compared to benign tissues (Fig. 3C). Additionally, in higher-stage groups (above Stage II), TROAP expression exceeded that in lower-stage groups (Stage II or below) (Fig. 3D). Survival analysis of cases with follow-up data revealed that higher TROAP expression was associated with shorter

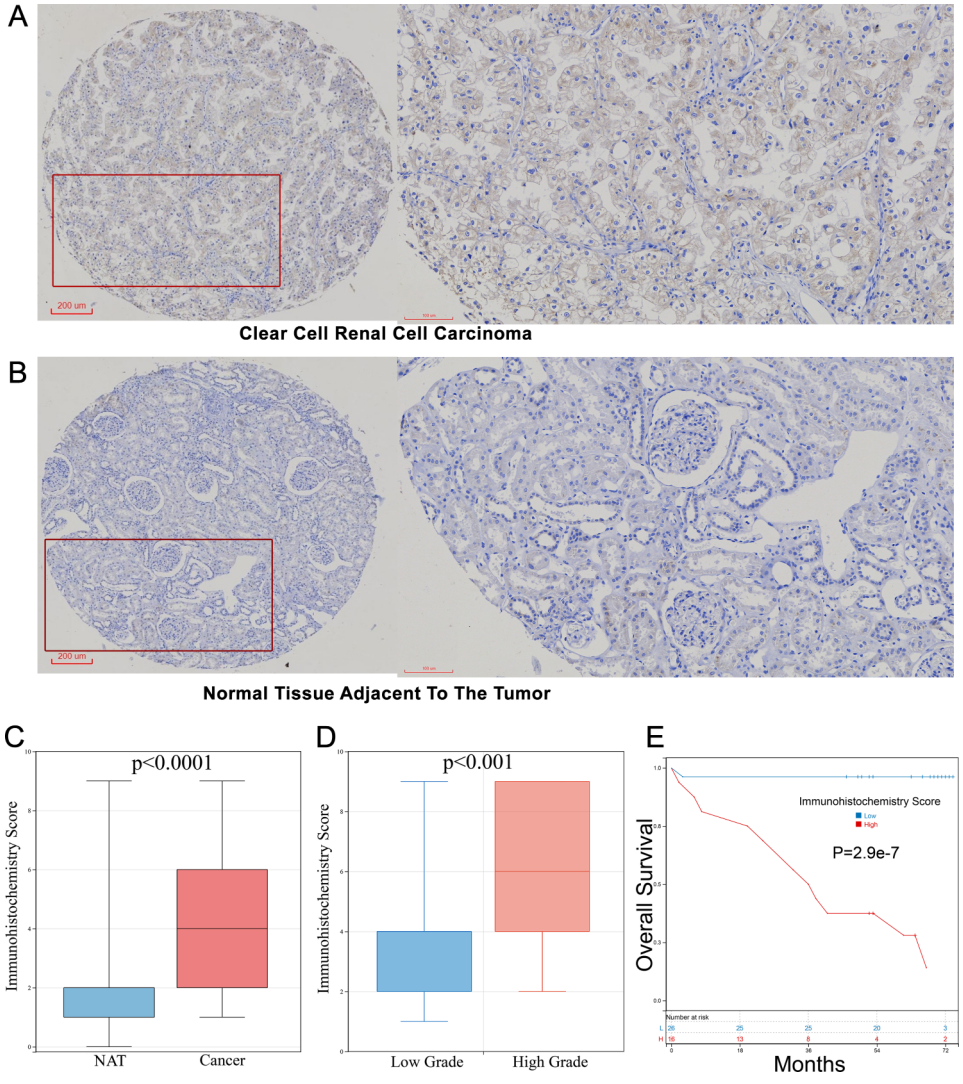

Fig. 3 Immunohistochemistry of TROAP expression in clinical samples. (**A**) Representative images of tumor tissues. (**B**) Representative images of benign tissues. (**C**) Scoring statistics for benign and tumor tissues. (**D**) Scoring statistics for low grade and high grade tissues. (**E**) Kaplan-Meier survival analysis

OS (Fig. 3E). These findings from the IHC align with our transcriptomic data.

Functional enrichment analysis

Following the elucidation of TROAP's prognostic importance in RCC, we further explored its potential biological roles. Employing Gene set enrichment analysis based on Hallmarks pathways, we displayed the top five pathways with the highest enrichment scores in three RCC subtypes (Fig. 4). Interestingly, across KIRC, KIRP, and KIRP, the pathways of E2F_TARGETS, G2M_CHECKPOINT and MYC_TARGETS were consistently enriched. These findings suggest that TROAP may exert an oncogenic effect in RCC.

Gene mutation regard to TROAP

In our transcriptomic-focused study, we analyzed the role of TROAP in relation to gene mutations. As depicted in Fig. 5A, in KIRC, mutation frequencies exceeding 20% were observed in three genes: VHL at 40%, PBRM1 at 41%, and TTN at 24%. In KICH, TP53 exhibited a notably high mutation frequency of 31%, with other genes showing frequencies below 10% (Fig. 5B). For KIRP, the highest mutation frequency was 19% for TTN, with others remaining below 10% (Fig. 5C). However, after grouping by the median expression levels of TROAP, most gene mutation frequencies showed no significant differences. Notable exceptions included a higher mutation frequency of BAP1 in the high TROAP expression group in KIRC, and a lower mutation frequency of LRP2 in the high TROAP expression group in KIRP. These findings

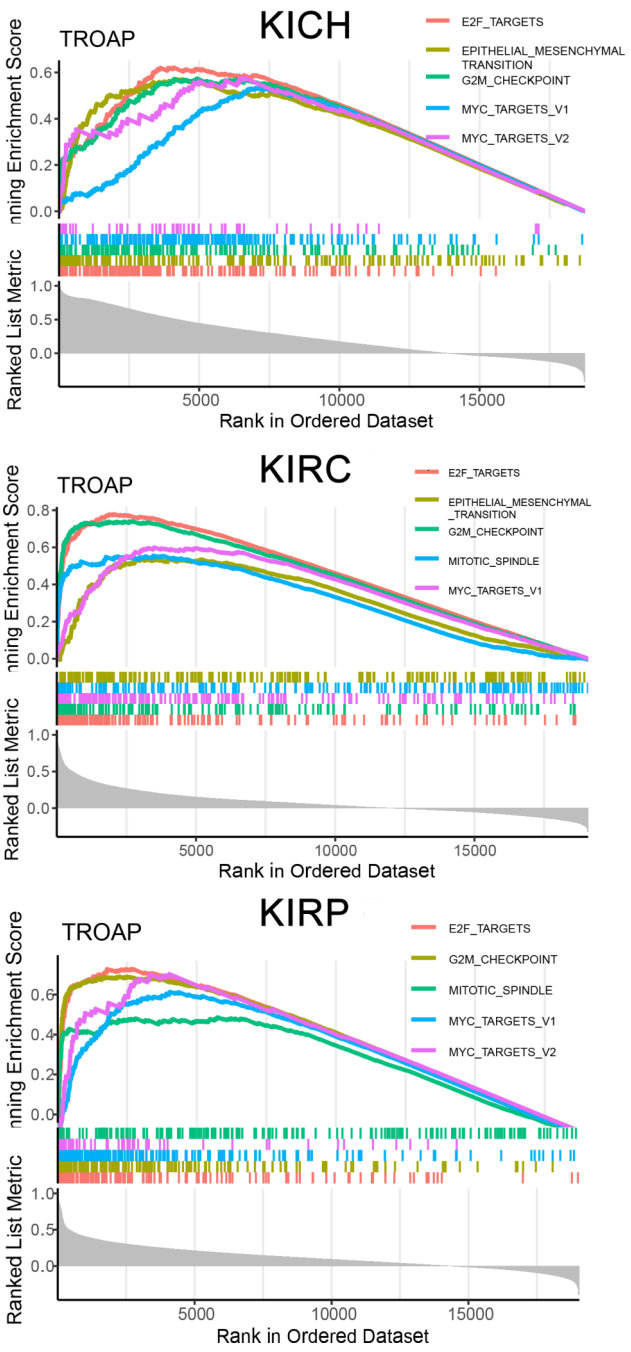

Fig. 4 Functional enrichment analysis of TROAP

suggest that TROAP's relationship with gene mutations in RCC may be limited.

TROAP is associated with poor therapeutic response

Upon establishing TROAP as an adverse prognostic factor in RCC, we endeavored to explore its correlation with the therapeutic response. In the advanced RCC cohort, we observed that patients with high TROAP expression exhibited poorer outcomes under nivolumab treatment, consistent across both OS and PFS metrics (Fig. 6A). Similarly, patients with high TROAP expression also showed worse prognosis in terms of PFS when treated with everolimus (Fig. 6A).

To further substantiate the connection between TROAP expression and immunotherapy response, we conducted submap analysis within the RCC cohorts. While results were statistically non-significant in the KICH cohort, a similar trend was noted elsewhere; lower TROAP expression was associated with a higher response rate to anti-PD-1 immunotherapy (Fig. 6B). These findings suggest TROAP's potential as a predictive marker for RCC immunotherapy and everolimus responses.

Additionally, we initiated a preliminary investigation into the mechanisms linking TROAP to immunotherapy response. Through xCELL immune infiltration analysis, we identified a significant negative correlation between TROAP and Th2 cells in RCC, indicating that TROAP may associated with the aberrant immune microenvironment in RCC (Fig. 7C).

Oncogene effect of TROAP in vitro

In our final series of experiments, we investigated the function of TROAP in RCC cell lines. Three si-RNA sequences targeting TROAP were designed and transfected into Caki-1 and 786-O cell lines. As illustrated in Fig. 7A, si-1 and si-2 demonstrated high knockdown efficiency, and were therefore chosen for further analysis. Following TROAP knockdown, a significant decrease in cellular proliferation was observed in the plate cloning assay (Fig. 7B). Likewise, cell viability was notably reduced in the CCK-8 assay after TROAP silencing (Fig. 7C). Moreover, the transwell migration assay showed a substantial reduction in cell migration capabilities upon TROAP depletion (Fig. 7D). These results collectively highlight the oncogene effect of TROAP in RCC cell lines.

Discussion

RCC represents the most prevalent malignant tumor of the upper urinary tract within the urinary system, constituting 3% of all adult malignancies [23, 24]. Advances in diagnostic and therapeutic techniques have elevated the 5-year survival rate for RCC to 74%, with advanced metastases occurring in only 12% of cases [25]. Beyond surgical interventions, other treatment approaches often fail to yield satisfactory outcomes. Consequently, identifying sensitive biomarkers and specific therapeutic targets for tailored treatment strategies holds critical clinical importance for enhancing the survival rates of RCC patients.

In this study, through multi-omics data and experimental validation, we have identified the potential of TROAP as a biomarker for RCC. Extensive research has

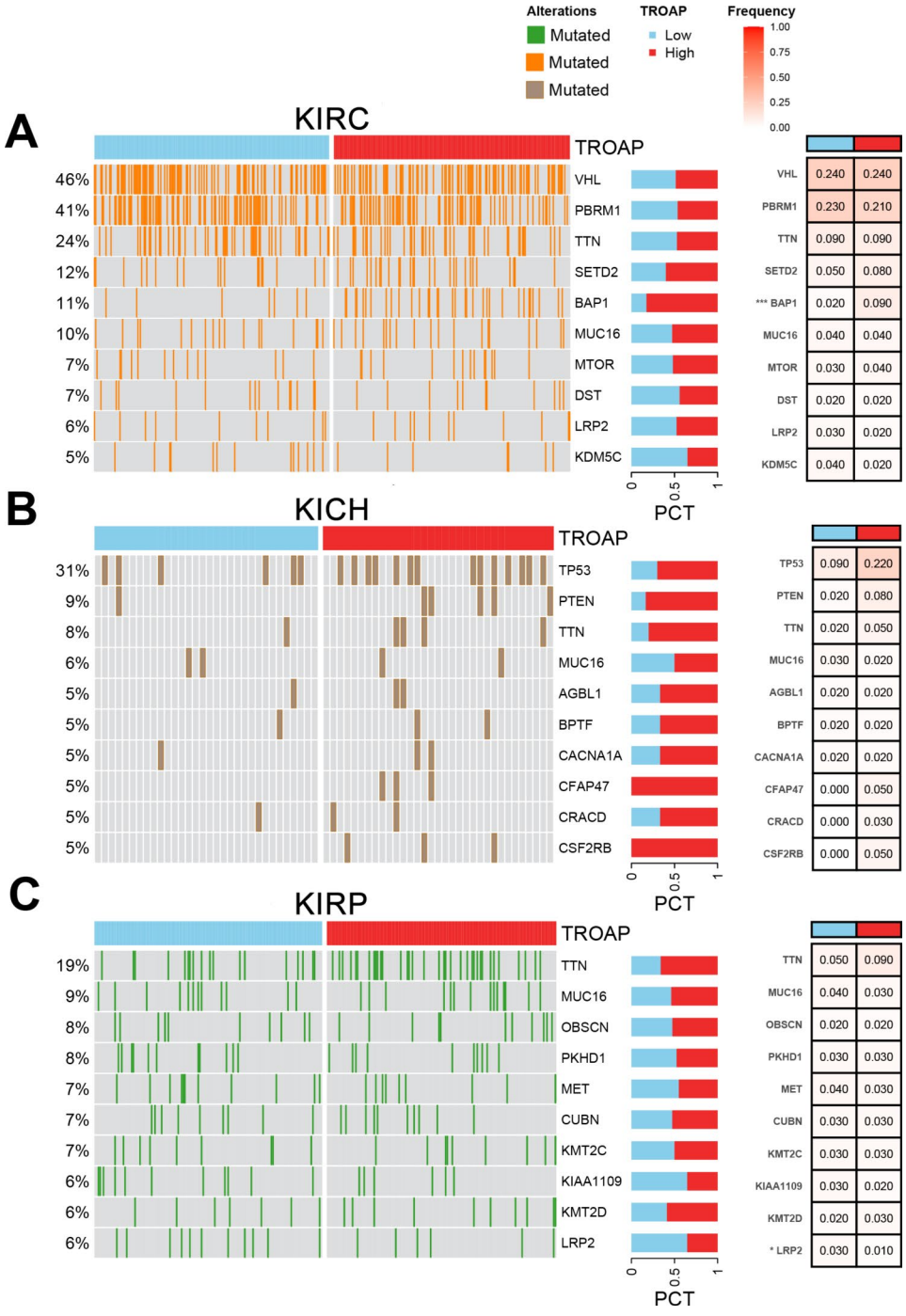

Fig. 5 Gene mutation landscape related to TROAP. (**A**) Renal Clear Cell Carcinoma. (**B**) Chromophobe. (**C**) Renal Papillary Cell Carcinoma. *$P < 0.05$; **$P < 0.01$; ***$P < 0.001$

demonstrated TROAP's elevated expression across various malignancies including prostate cancer [26], breast cancer [27], colorectal cancer [28], hepatocellular carcinoma [29], and gastric cancer [30]. Han Liu and colleagues have elucidated that TROAP modulates the cell division cycle 20 (CDC20) and affects spindle microtubules (ASPM), thereby facilitating malignant tumor progression during the S and G2 phases of the cell cycle [31]. Additionally, TROAP has been shown to influence tumor progression through diverse pathways, such as enhancing disease advancement via the Wnt3/survival protein signaling pathway in prostate cancer [26]. Notably, TROAP expression is positively associated with clinical severity in hepatocellular carcinoma, which correlates

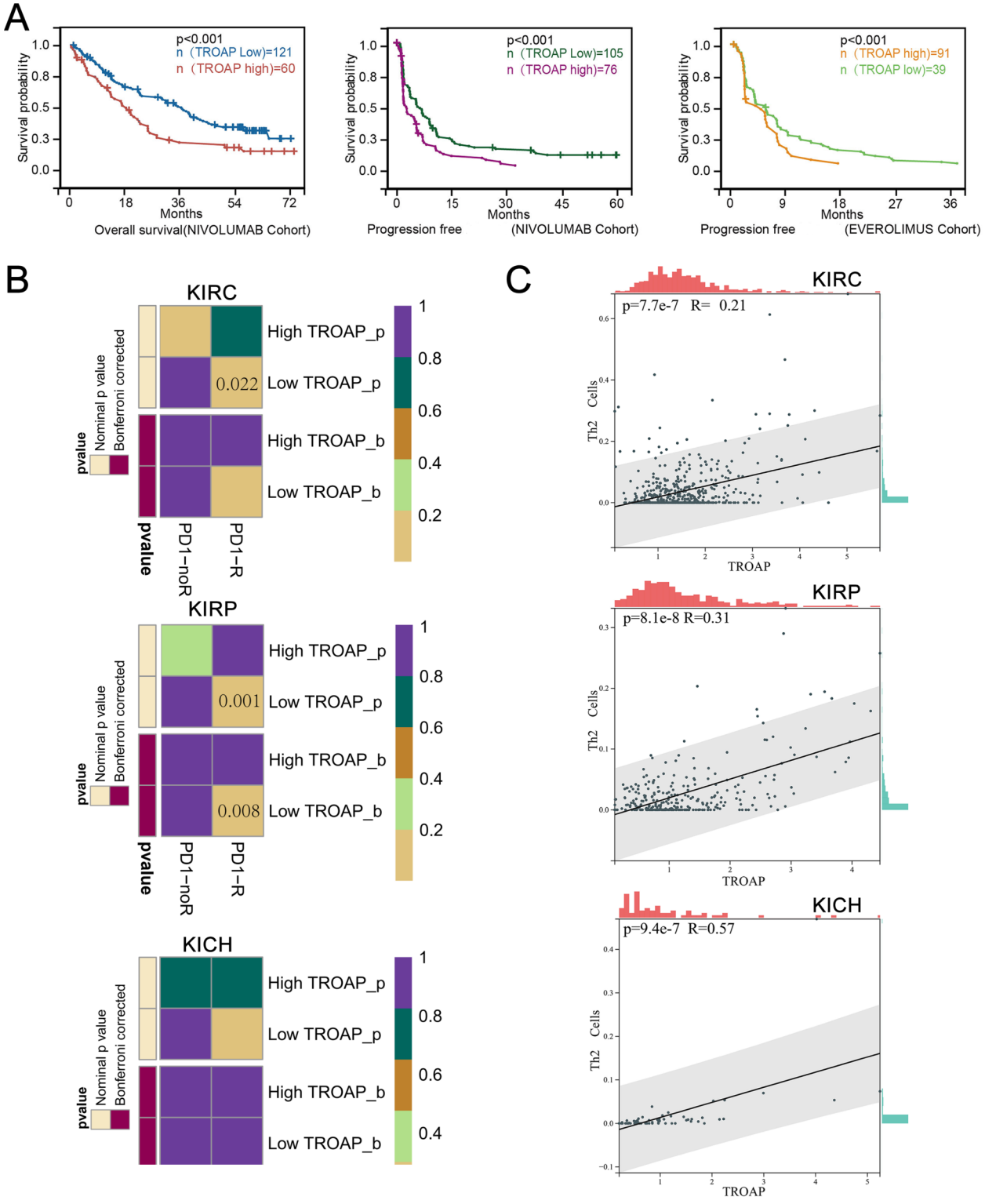

Fig. 6 TROAP is a biomarker for therapy response in RCC. (**A**) Survival analysis of TROAP in advanced RCC cohorts. (**B**) Submap analysis forecasting immunotherapy response across pan-RCC. (**C**) Correlation between TROAP expression and Th2 cell in pan-RCC

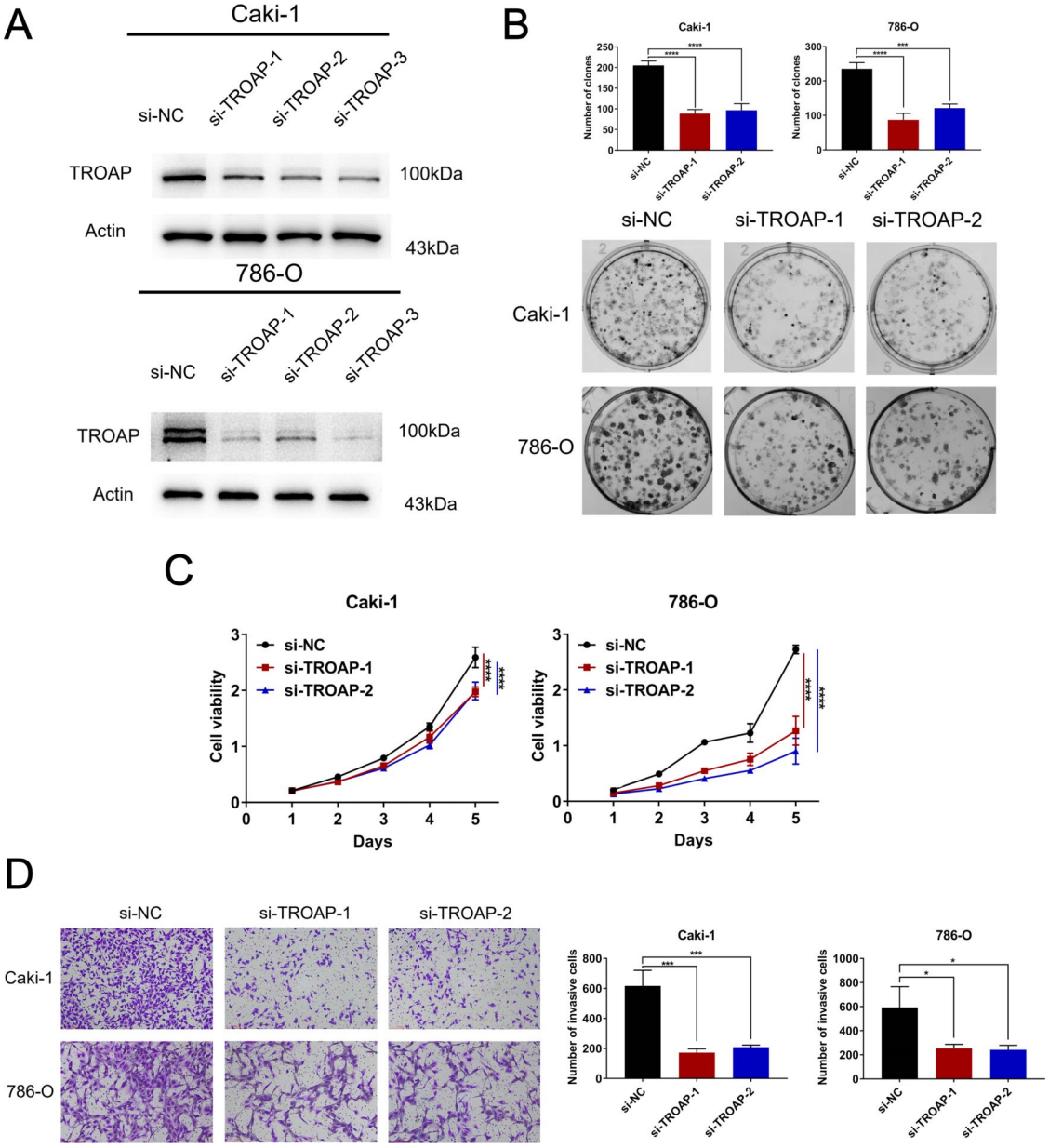

Fig. 7 Oncogene effect of TROAP in vitro. (**A**) Western blot analysis was employed to evaluate the effectiveness of TROAP silencing in Caki-1 and 786-O cell lines. (**B**) Clone formation to determine the colony-forming ability of Caki-1 and 786-O cell lines. (**C**) The CCK-8 assay was conducted to measure the proliferation rates of Caki-1 and 786-O cell lines. (**D**) Transwell assays were performed to assess the invasive potential of Caki-1 and 786-O cell lines. *$P<0.05$; **$P<0.01$; ***$P<0.001$;****$P<0.0001$

with poorer overall and disease-free survival [29]. These findings are consistent with our observations in RCC.

Furthermore, we observed that TROAP expression is relatively lower in RCC compared to most other cancers. We hypothesize two potential reasons for this phenomenon. Firstly, TROAP may exhibit tissue specificity. As shown in Fig. 1A, the top three cancers with the highest TROAP expression are Testicular Germ Cell Tumors (TGCT), Cervical squamous cell carcinoma and endocervical adenocarcinoma (CESC) and Uterine Carcinosarcoma (UCS), all of which are tumors of the reproductive system. Secondly, gene mutations often influence mRNA expression. However, our multi-omics analysis indicates that TROAP's relationship with gene mutations in RCC may be limited. This could also contribute to the lower expression of TROAP in RCC compared to other cancers. The above perspectives are preliminary hypotheses. We plan to validate these ideas through more comprehensive experiments and analyses in our future work.

In our functional enrichment analysis, the pathways E2F_TARGETS, G2M_CHECKPOINT, and MYC_TARGETS were consistently enriched across KIRC, KIRP and

KICH. E2F1, which has been extensively studied in RCC, exhibits dual functions in VHL-defective renal cell carcinoma, largely depending on the balance between HIF1α and HIF2α. It appears that E2F1 may act oncogene effect in advanced tumors predominantly expressing HIF2α, while functioning as a tumor suppressor in others [32]. The G2M checkpoint is crucial for maintaining genomic stability by ensuring DNA integrity and blocking the mitotic progression of cells with compromised DNA. Alterations in the G2M checkpoint or its downstream signaling pathways can influence cancer progression and may provide markers for assessing tumor behavior, response to treatment, or prognosis [33]. Additionally, targeting the G2M checkpoint might offer therapeutic opportunities to enhance the sensitivity of cancer cells to DNA-damaging agents or to selectively trigger apoptosis in ccRCC with defective DNA repair mechanisms [34]. Similarly, other research groups have recognized the clinical significance of MYC pathways in renal cancer [35]. Therefore, our findings are corroborated by other studies, further validating the significant role of in RCC.

Additionally, we validated TROAP's function within RCC cell lines, despite previous reports by Wang et al. detailing cell assays on TROAP [15]. Our study employed different cell lines and experimental techniques, enhancing our understanding of TROAP in vitro. More significantly, we reported for the first time that TROAP can serve as a biomarker for the response to RCC pharmacotherapy. Nivolumab and everolimus are critical components of the therapeutic regimen for advanced RCC, and our results contribute new evidence supporting the clinical translational potential of TROAP.

Furthermore, we conducted a preliminary analysis of the mechanisms by which high TROAP expression correlates with poor immunotherapy response. Through immune cell infiltration analysis in three RCC contexts, we found a positive correlation between TROAP expression and Th2 cell infiltration. Research indicates that inhibiting Th2 cells during immunotherapy can significantly bolster the host immune response and inhibit tumor growth [36]. Suppression of Th2 cytokines has been shown to enhance the infiltration and proliferation of cytotoxic CD8+T cells, and to increase their secretion of cytotoxic cytokines, thereby activating antitumor T cell immunity [37].

However, this study recognizes several limitations. Constraints in time restricted a thorough mechanistic investigation of TROAP's function in RCC. Planned future studies aim to systematically explore and amend these limitations.

In conclusion, our research underscores the critical role of TROAP in RCC, establishing its potential as a biomarker for prognosis and therapeutic response.

Abbreviations

ACC	Adrenocortical carcinoma
ASPM	Affects spindle microtubules
AUC	Area under the curve
BLCA	Bladder urothelial carcinoma
BRCA	Breast invasive carcinoma
CDC20	Cell division cycle 20
CESC	Cervical squamous cell carcinoma and endocervical adenocarcinoma
CHOL	Cholangiocarcinoma
COAD	Colon adenocarcinoma
DLBC	Lymphoid neoplasm diffuse large B-cell lymphoma
ESCA	Esophageal carcinoma
GBM	Glioblastoma multiforme
GEO	Gene Expression Omnibus
GSEA	Gene Set Enrichment Analysis
HNSC	Head and neck squamous cell carcinoma
IHC	Immunohistochemistry
KICH	Chromophobe renal cell carcinoma
KIRC	Renal clear cell carcinoma
KIRP	Papillary renal cell carcinoma
KM	Kaplan-Meier
LAML	Acute myeloid leukemia
LGG	Brain lower grade glioma
LIHC	Liver hepatocellular carcinoma
LUAD	Lung adenocarcinoma
LUSC	Lung squamous cell carcinoma
MESO	Mesothelioma
NAT	Normal tissue adjacent to the tumor
NC	Negative control
OD	Optical density
OS	Overall survival
OV	Ovarian cancer
PAAD	Pancreatic adenocarcinoma
PBS	Phosphate-buffered saline
PCPG	Pheochromocytoma and paraganglioma
PFI	Progression Free Interval
PRAD	Prostate adenocarcinoma
RCC	Renal cell carcinoma
READ	Rectum adenocarcinoma
ROC	Receiver operating characteristic
SARC	Sarcoma
SKCM	Skin cutaneous melanoma
STAD	Stomach adenocarcinoma
STR	Short tandem repeat
TCGA	The Cancer Genome Atlas
TGCT	Testicular germ cell tumor
Th2	Type 2T helper
THCA	Thyroid carcinoma
THYM	Thymoma
TROAP	Trophinin associated protein
UCEC	Uterine corpus endometrial carcinoma
UCS	Uterine carcinosarcoma
UVM	Uveal melanoma

Supplementary Information

The online version contains supplementary material available at https://doi.org/10.1186/s12885-024-12802-9.

Supplementary Material 1

Supplementary Material 2

Supplementary Material 3

Acknowledgements

The authors express their sincere appreciation to the TCGA (The Cancer Genome Atlas) and GEO (Gene Expression Omnibus) databases for making multi-omics data publicly available, which has substantially aided the research conducted in this study.

Author contributions
Yifen Wu played a pivotal role in securing funding and designing the study. The public datasets collection and analysis were diligently conducted by Qinglin Tan, Peiliang Kong, Guobiao Chen, Yanmin Cai, and Kejun Liu. The initial draft of the manuscript was prepared by Qinglin Tan, Peiliang Kong, Chen Chen, Huiting Mo and Yuancheng Huang. The immunohistochemistry and cell assays was completed by Qinglin Tan and Guobiao. The manuscript underwent thorough refinement and revision by Yifen Wu and Jianming Lu. Each author made significant contributions to the development of the article and has given their approval for the final version.

Funding
Guangdong Basic and Applied Basic Research Foundation (Project's number: 2020B1515120063).

Data availability
The datasets utilized in this study has been delineated within the Materials and Methods section. For any further inquiries, please reach out to the corresponding author.

Declarations

Ethics approval and consent to participate
The procurement of clinical samples was conducted with ethical approval from the Ethics Committee of Shanghai Zhuoli Biotech Company (approval number SHLLS-BA-22101102).

Consent for publication
Not applicable.

Competing interests
The authors declare no competing interests.

Received: 26 May 2024 / Accepted: 13 August 2024
Published online: 17 August 2024

References

1. Lv D, Zhou H, Cui F, et al. Characterization of renal artery variation in patients with clear cell renal cell carcinoma and the predictive value of accessory renal artery in pathological grading of renal cell carcinoma: a retrospective and observational study. BMC Cancer. 2023;23:274.
2. Sung H, Ferlay J, Siegel RL, et al. Global Cancer statistics 2020: GLOBOCAN estimates of incidence and Mortality Worldwide for 36 cancers in 185 countries. CA Cancer J Clin. 2021;71:209–49.
3. Liu Y, Zhang Z, Xi P, et al. Systematic analysis of RNASET2 gene as a potential prognostic and immunological biomarker in clear cell renal cell carcinoma. BMC Cancer. 2023;23:837.
4. Shuch B, Amin A, Armstrong AJ, et al. Understanding pathologic variants of renal cell carcinoma: distilling therapeutic opportunities from biologic complexity. Eur Urol. 2015;67:85–97.
5. Schödel J, Grampp S, Maher ER, et al. Hypoxia, hypoxia-inducible transcription factors, and Renal Cancer. Eur Urol. 2016;69:646–57.
6. Zhang B, Han D, Yang L, et al. The mitochondrial fusion-associated protein MFN2 can be used as a novel prognostic molecule for clear cell renal cell carcinoma. BMC Cancer. 2023;23:986.
7. Mollica V, Di Nunno V, Massari F. Pembrolizumab plus Axitinib: a new treatment option for patients with metastatic renal cell carcinoma. Chin Clin Oncol. 2019;8:S21.
8. Wang LH, Cao B, Li YL, et al. Potential prognostic and therapeutic value of ANXA8 in renal cell carcinoma: based on the comprehensive analysis of annexins family. BMC Cancer. 2023;23:674.
9. Harshman LC, Xie W, Bjarnason GA, et al. Conditional survival of patients with metastatic renal-cell carcinoma treated with VEGF-targeted therapy: a population-based study. Lancet Oncol. 2012;13:927–35.
10. Du L, Wang B, Wu M, et al. LINC00926 promotes progression of renal cell carcinoma via regulating miR-30a-5p/SOX4 axis and activating IFNγ-JAK2-STAT1 pathway. Cancer Lett. 2023;578:216463.
11. Yang S, Liu X, Yin Y, et al. Tastin is required for bipolar spindle assembly and centrosome integrity during mitosis. Faseb j. 2008;22:1960–72.
12. Fukuda MN, Sato T, Nakayama J, et al. Trophinin and tastin, a novel cell adhesion molecule complex with potential involvement in embryo implantation. Genes Dev. 1995;9:1199–210.
13. Suzuki N, Nakayama J, Shih IM, et al. Expression of trophinin, tastin, and bystin by trophoblast and endometrial cells in human placenta. Biol Reprod. 1999;60:621–7.
14. Suzuki N, Zara J, Sato T, et al. A cytoplasmic protein, bystin, interacts with trophinin, tastin, and cytokeratin and may be involved in trophinin-mediated cell adhesion between trophoblast and endometrial epithelial cells. Proc Natl Acad Sci U S A. 1998;95:5027–32.
15. Wang J, Wan H, Mi Y et al. TROAP promotes the Proliferation, Migration, and Metastasis of Kidney Renal Clear Cell Carcinoma with the help of STAT3. Int J Mol Sci 2023;24.
16. Braun DA, Hou Y, Bakouny Z, et al. Interplay of somatic alterations and immune infiltration modulates response to PD-1 blockade in advanced clear cell renal cell carcinoma. Nat Med. 2020;26:909–18.
17. Liao C, Wang X. TCGAplot: an R package for integrative pan-cancer analysis and visualization of TCGA multi-omics data. BMC Bioinformatics. 2023;24:483.
18. Yu G, Wang LG, Han Y, et al. clusterProfiler: an R package for comparing biological themes among gene clusters. Omics. 2012;16:284–7.
19. Yin W, Chen G, Li Y, et al. Identification of a 9-gene signature to enhance biochemical recurrence prediction in primary prostate cancer: a benchmarking study using ten machine learning methods and twelve patient cohorts. Cancer Lett. 2024;588:216739.
20. Zeng D, Ye Z, Shen R, et al. IOBR: Multi-omics Immuno-Oncology Biological Research to Decode Tumor Microenvironment and signatures. Front Immunol. 2021;12:687975.
21. Liu R, Zou Z, Chen L, et al. FKBP10 promotes clear cell renal cell carcinoma progression and regulates sensitivity to the HIF2α blockade by facilitating LDHA phosphorylation. Cell Death Dis. 2024;15:64.
22. Mayakonda A, Lin DC, Assenov Y, et al. Maftools: efficient and comprehensive analysis of somatic variants in cancer. Genome Res. 2018;28:1747–56.
23. Singh A, Choudhury SD, Singh P, et al. Disruption in networking of KCMF1 linked ubiquitin ligase impairs autophagy in CD8(+) memory T cells of patients with renal cell carcinoma. Cancer Lett. 2023;564:216194.
24. Chen WJ, Pan XW, Song X, et al. Preoperative neoadjuvant targeted therapy remodels intra-tumoral heterogeneity of clear-cell renal cell carcinoma and ferroptosis inhibition induces resistance progression. Cancer Lett. 2024;593:216963.
25. Siegel RL, Miller KD, Wagle NS, et al. Cancer statistics, 2023. CA Cancer J Clin. 2023;73:17–48.
26. Ye J, Chu C, Chen M, et al. TROAP regulates prostate cancer progression via the WNT3/survivin signalling pathways. Oncol Rep. 2019;41:1169–79.
27. Li K, Zhang R, Wei M, et al. TROAP promotes breast Cancer Proliferation and Metastasis. Biomed Res Int. 2019;2019:6140951.
28. Ye X, Lv H. MicroRNA-519d-3p inhibits cell proliferation and migration by targeting TROAP in colorectal cancer. Biomed Pharmacother. 2018;105:879–86.
29. Li L, Wei JR, Song Y, et al. TROAP switches DYRK1 activity to drive hepatocellular carcinoma progression. Cell Death Dis. 2021;12:125.
30. Cardillo TM, Govindan SV, Sharkey RM, et al. Sacituzumab Govitecan (IMMU-132), an Anti-Trop-2/SN-38 antibody-drug Conjugate: characterization and efficacy in pancreatic, gastric, and other cancers. Bioconjug Chem. 2015;26:919–31.
31. Liu H, Zhou Q, Xu X, et al. ASPM and TROAP gene expression as potential malignant tumor markers. Ann Transl Med. 2022;10:586.
32. Tian W, Cui F, Esteban MA. E2F1 in renal cancer: Mr Hyde disguised as Dr Jekyll? J Pathol. 2013;231:143–6.
33. Wang Z, Zheng Z, Wang B, et al. Characterization of a G2M checkpoint-related gene model and subtypes associated with immunotherapy response for clear cell renal cell carcinoma. Heliyon. 2024;10:e29289.
34. Huang X, Huang Y, Lv Z et al. Loss of cell division cycle–associated 5 promotes cell apoptosis by activating DNA damage response in clear cell renal cell carcinoma. Int J Oncol 2022;61.
35. Priyam J, Saxena U. Stage-specific coexpression network analysis of Myc in cohorts of renal cancer. Sci Rep. 2023;13:11848.
36. Saulite I, Ignatova D, Chang YT, et al. Blockade of programmed cell death protein 1 (PD-1) in Sézary syndrome reduces Th2 phenotype of non-tumoral T lymphocytes but may enhance tumor proliferation. Oncoimmunology. 2020;9:1738797.

37. Loeuillard E, Yang J, Buckarma E, et al. Targeting tumor-associated macrophages and granulocytic myeloid-derived suppressor cells augments PD-1 blockade in cholangiocarcinoma. J Clin Invest. 2020;130:5380–96.

Publisher's Note